

---

## Removal of metals using a ZnO/Au composite under visible-light illumination

Thonglim P., Sirivichai M., Thanjai O. and Locharoenrat K.

Department of Physics, Faculty of Science, King Mongkut's Institute of Technology Ladkrabang, Bangkok 10520, Thailand, kitsakorn.lo@kmitl.ac.th

**Received:** 02.10.2017

**Abstract.** Gold nanoparticles embedded into a ZnO film are prepared with a simple spin-coating technique. Photocatalytic performance of the film is studied under irradiation with the visible light. We suggest to increase the amount of Au nanoparticles in the ZnO matrix (from 0 to 400 mg in our particular case) to improve photocatalytic efficiency of the film via a combination of plasmonic-resonance and Schottky-barrier effects. We choose  $\text{Fe}^{2+}$  as a model representative of metals available in the wastewater. It is demonstrated that the ZnO/Au films with increased Au content reduce efficiently the amount of ferrum ions in the water solution. In particular, the film with the content ratio ZnO:Au = 1:2 serves as a good absorber for removing  $\text{Fe}^{2+}$  in case if their initial concentration is equal to 0.2 mM.

**Keywords:** nanoparticles, photocatalysts, plasmonics, semiconductors, Schottky structures

**PACS:** 77.55.Hf, 78.40.Fy, 78.40.Kc, 78.67.Bf

**UDC:** 535.343

### 1. Introduction

Wastewater and water contamination represent a global issue for natural seas and rivers. Groundwater is also polluted by heavy metals originating from both electronic and heavy industries. In this respect, removal of heavy metals as water pollutants with the aid of photocatalytic materials under sunlight is a promising 'green' way out. Nanoscaled semiconductor photocatalysts, e.g. ZnO, have recently been suggested to improve photocatalytic efficiencies, since nanoparticles are characterized by enormous surface-to-volume ratio, thus allowing higher adsorption of the target molecules [1]. This means that interactions of the nanoparticles and surrounding media affect essentially the emission spectrum. Furthermore, the nanoparticles are attractive for water purification since they are capable of removing biological contaminants, besides of simple chemicals. For instance, it is known that  $\text{TiO}_2$  enhances antibacterial effect [2–5], whereas  $\text{WO}_3$  can be efficiently used to eliminate organic pollutants [6–9].

In principle, semiconductor photocatalysts absorb light more or less efficiently in the visible and near-ultraviolet ranges, provided that a sufficient number of vacant electronic states are present to inhibit recombination of electron-hole pairs upon light exposure. Moreover, plasmonic photocatalysis has recently facilitated a rapid progress in enhancing the photocatalytic efficiency under visible-light irradiation, increasing the prospects of sunlight for environmental and energy applications, such as wastewater treatment, water splitting and carbon dioxide reduction. The plasmonic photocatalysis makes use of noble metals dispersed in semiconductor photocatalysts. For example, Zhang et al. have studied application of Au/ $\text{TiO}_2$  suspension in water to produce 0.71% hydrogen under a simulated sunlight illumination [10]. Xianming et al. have reported that ZnO/Au suspension in water, under ultraviolet irradiation, can be applied to degrade

Rhodamine B [11]. Under the white light, ZnO/Au suspension in water degrades Rhodamine 6G and Thionine [12]. Moreover, Yiqiang et al. have shown that, under the same conditions, this suspension degrades the other organic dyes [13]. It has been revealed that the plasmonic effect enhances the excitation energy of electron–hole pairs in semiconductors. Scattering of resonant photons also increases a length of average photon path in these composite photoactive materials.

Since then, many semiconductor photocatalysts have been prepared as suspensions in water and mixed with various kinds of organic pollutants to understand the mechanisms of their photocatalytic activity via the plasmonic effect. Nonetheless, we do not know of the literature associated with the studies of ZnO/Au in a form of thin films or with their applications to such inorganic pollutants as metals, for which the improvement of photocatalytic activity should involve some additional mechanisms. Hence, there is a clear need in focusing on this material.

Since ZnO has a photocatalytic optical bandgap in the ultraviolet-visible range, plasmon-enhanced photochemical efficiency seems to be possible for this system. In this report, we implement highly efficient plasmonic photocatalysis in order to remove metals from the wastewater. For this aim, we deposit ZnO/Au nanocomposites in a polymer matrix onto a glass substrate, using a standard spin-coating route. Next we study the effect of concentration of the plasmonic crystal on the photocatalytic degradation of a particular metal,  $\text{Fe}^{2+}$ , under illumination with the visible light. We also formulate a protocol for fabricating highly photoactive photocatalysts. Two prominent features are purposed, a Schottky junction and a localized surface plasmonic resonance [14, 15]. The former yields benefits in charge separation and transfer, whereas the latter contributes to a strong absorption of visible light and excitation of active charge carriers.

## 2. Experimental

### 2.1. Materials

Regarding the necessary initial materials, we purchased an Au nanopowder (with the particle diameters  $100\pm 10$  nm), ZnO nanopowder (with the diameters  $50\pm 5$  nm) and a polymethymethacrylate powder from Sigma Aldrich (USA).  $\text{FeCl}_2$  was ordered from Fluka (Japan). Finally, dichloromethane was bought from Carlo Erba (Thailand).

### 2.2. Preparation of ZnO/Au film

ZnO/Au films were synthesized using a known spin-coating technique. First, 100 mg of ZnO and 0.2 g of polymethymethacrylate powder were mixed with different amounts of Au in 1 ml of dichloromethane for 2 h, under the conditions of ultrasonic bath (see Table 1).

Table 1. Parameters specifying fabrication of ZnO/Au films.

Polymethymethacrylate powder	ZnO	Au	Dichloromethane	Molar ratio(ZnO: Au)
0.2 g	100 mg	0 mg	1 ml	1:0
0.2 g	100 mg	100 mg	1 ml	1:0.5
0.2 g	100 mg	200 mg	1 ml	1:1
0.2 g	100 mg	400 mg	1 ml	1:2

The mixed solution was spread onto a glass substrate with the dimensions  $3.5 \times 2.0 \times 0.1 \text{ cm}^3$ . It was spun using a spin-coater at the rotation speed of 3500 rpm for 5 s to finally achieve ZnO/Au films with a number of ZnO-to-Au ratios: 1:0, 1:0.5, 1:1 and 1:2.

### 2.3. Photocatalytic performance

The films with the above ZnO/Au ratios were dipped into 16 ml of 0.2 mM  $\text{Fe}^{2+}$  solution. Note that the  $\text{Fe}^{2+}$  solution was conveniently used as a representative of metals in the wastewater. According to the standards associated with wastewater treatment, the amounts of  $\text{Fe}^{2+}$  should not go over 0.2 mM. The surface of each film was 1 mm apart from the surface of  $\text{Fe}^{2+}$  solution. A fluorescent lamp served as a substitute for sunlight. It was installed 80 cm from the solution surface. The film was left in the solution under illumination that lasted for 90 min. A scheme used for testing the photocatalytic activity under the room temperature and the light illuminance of 529.67 lux is shown in Fig. 1.

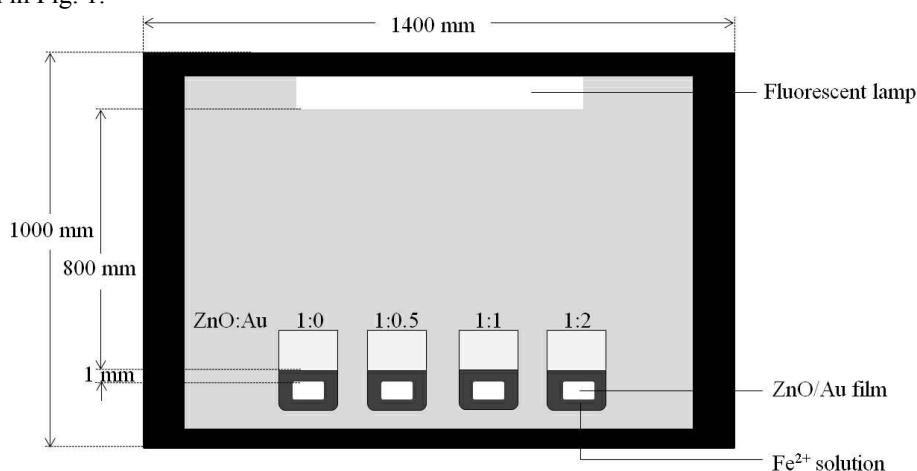


**Fig. 1.** Setup for studying photocatalysis.

A resultant  $\text{Fe}^{2+}$  solution and a dipped film were transferred separately to sample holders to check their optical absorption with a UV-Vis spectrometer (the model Avantes 0905032E1). A tungsten lamp emitting in the wavelength region 300–700 nm was used as a light source (see Fig. 2).

Reduction of  $\text{Fe}^{2+}$  concentration was determined by the ratio  $C/C_0$ , where  $C_0 = 0.2 \text{ mM}$  and  $C$  are the  $\text{Fe}^{2+}$  concentrations respectively before and after the film was dipped into the  $\text{Fe}^{2+}$  solution. The  $C$  parameter was calculated indirectly, using a standard curve known for the stock  $\text{Fe}^{2+}$

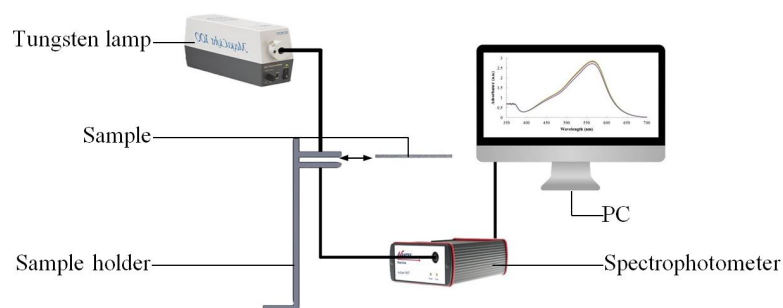


**Fig. 2.** Our optical setup.

solutions. This curve was plotted using different concentrations of the stock  $\text{Fe}^{2+}$  solutions, where the absorbance was measured at 560 nm. Fig. 3 displays also the corresponding polynomial fit,  $y = -0.396x^2 + 1.490x + 2.497$ . Then the amount of  $\text{Fe}^{2+}$  unattached to the film surface ( $C$  or  $x$ ) can easily be calculated, provided that we know a priori the absorption-peak intensity for the resultant amount of  $\text{Fe}^{2+}$  in the solution after the film is dipped into the solution (the quantity denoted here as  $y$ ).

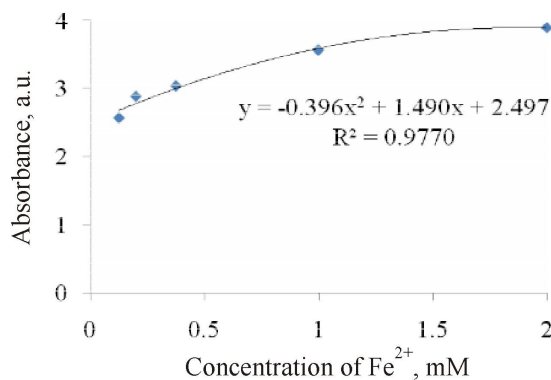


**Fig. 3.** Absorbance of a standard sample of stock  $\text{Fe}^{2+}$  as a function of its concentration.

#### 2.4. Film characterization

Surface morphology of each of our ZnO/Au films was characterized under a microscope with the magnification  $10^{\times}$  (the model Nikon ECLIPSE E200).

### 3. Results and discussion

Since the amount of gold nanoparticles varies from 0 to 400 mg at a fixed amount of ZnO nanoparticles, the ZnO:Au ratios in the ZnO/Au film under study are equal to 1:0, 1:0.5, 1:1 and 1:2. Fig. 4 shows the optical absorption of the films with different ZnO:Au ratios, which are measured before the films are dipped into the  $\text{Fe}^{2+}$  solution.

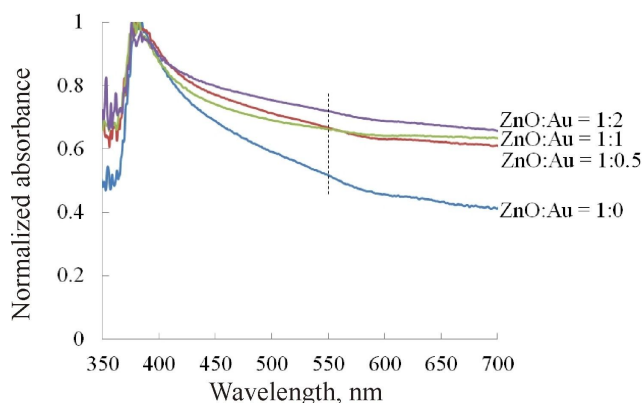


**Fig. 4.** Absorbance spectra of ZnO/Au films as functions of light wavelength, as measured before the films are dipped into  $\text{Fe}^{2+}$  solution.

The main peak corresponding to ZnO is located approximately at the wavelength of 380 nm, while a shoulder indicating to the presence of Au can be tested at about 550 nm. The spectrum seems to become broadened when the ZnO:Au ratio increases, so that the shoulder becomes more

pronounced in the visible range. This broadening can be naturally associated with still larger amounts of Au added to the ZnO matrix.

Fig. 5 displays the optical absorption of the ZnO/Au films obtained after the films are dipped into the  $\text{Fe}^{2+}$  solution. We remind that the latter solution, with the invariable concentration of 0.2 mM, serves here as a conventional representative of heavy metals in the wastewater. The main absorbance peaks seen from Fig. 5 are displayed separately in Fig. 6.

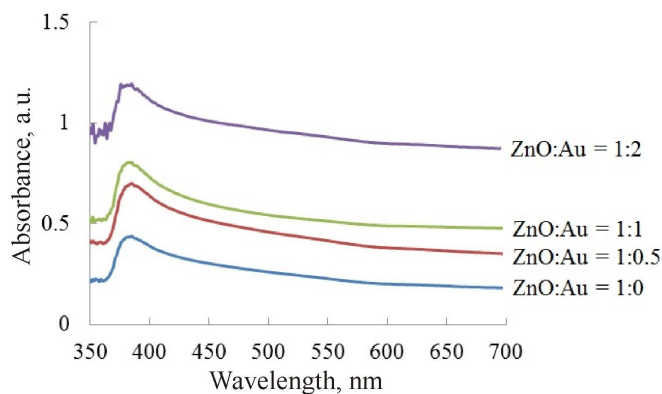


**Fig. 5.** Absorbance spectra of ZnO/Au films as functions of light wavelength, as measured after the films are dipped into  $\text{Fe}^{2+}$  solution.

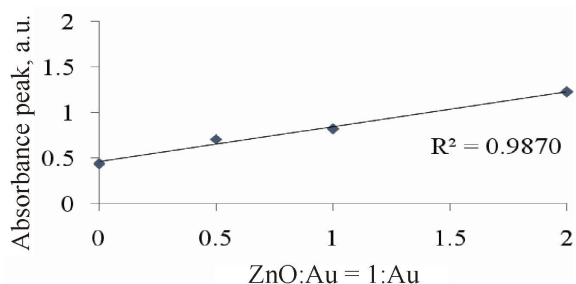


**Fig. 6.** Absorbance peak for ZnO/Au films as a function of ZnO:Au ratio, as calculated after the films are dipped into  $\text{Fe}^{2+}$  solution.

When the amount of Au increases, due to increasing ZnO:Au ratio from 1:0 up to 1:2, more and more  $\text{Fe}^{2+}$  forms on the ZnO/Au film [See our further discussion on the surface morphology of the films]. This implies that one can expect decreasing resultant  $\text{Fe}^{2+}$  amount in the solution. To confirm this point, we have further investigated the optical absorption of the resultant  $\text{Fe}^{2+}$  amount in the solution after the films are dipped into the solution (see Fig. 7). The corresponding absorbance peaks from Fig. 7 are displayed separately in Fig. 8.

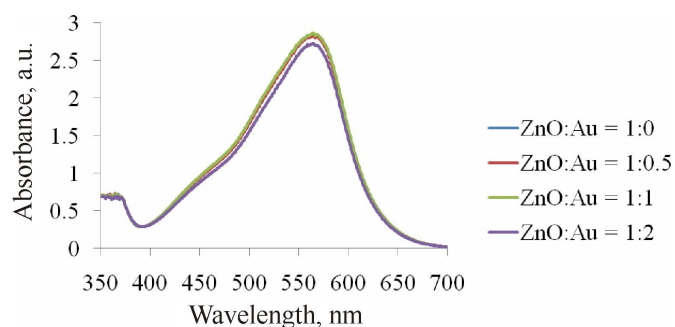


**Fig. 7.** Absorbance spectra of the resultant  $\text{Fe}^{2+}$  amounts in the  $\text{Fe}^{2+}$  solution as functions of wavelength, as measured after the ZnO/Au films are dipped into the solution.

It can be easily confirmed that the resultant  $\text{Fe}^{2+}$  amount in the  $\text{Fe}^{2+}$  solution decreases when the Au amount increases, due to increasing ZnO:Au ratio from 1:0 to 1:2. Following from the absorption peaks of Fig. 7, one can calculate the resultant  $\text{Fe}^{2+}$  concentration, using the standard

curve for the stock  $\text{Fe}^{2+}$  solution shown in Fig. 3. The ratio of the ‘resultant’  $\text{Fe}^{2+}$  concentration ( $C$ ) and its ‘initial’ concentration (i.e.,  $C_0 = 0.2$  mM) is plotted in Fig. 9 as a function of ZnO:Au ratio.

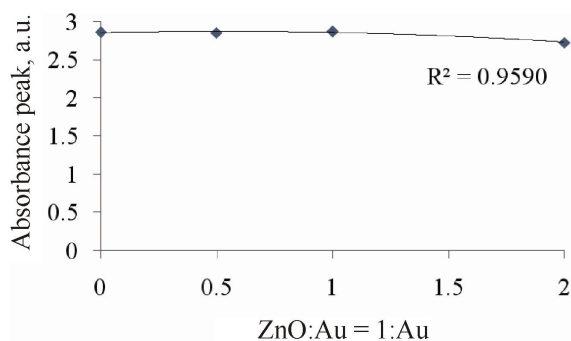


**Fig. 8.** Absorbance peak of the resultant  $\text{Fe}^{2+}$  amounts in the solution as a function of ZnO:Au ratio, as calculated after the ZnO/Au films are dipped into the solution.

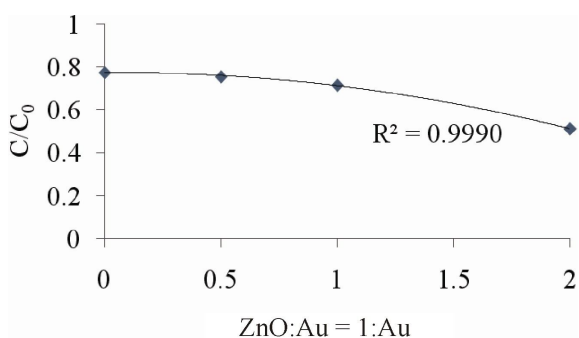


**Fig. 9.** Reduction of  $\text{Fe}^{2+}$  concentration ( $C/C_0$ ), which occurs after the ZnO/Au films are dipped into  $\text{Fe}^{2+}$  solution, as a function of ZnO:Au ratio.  $C_0$  and  $C$  denote  $\text{Fe}^{2+}$  concentrations respectively before and after the films are dipped into the solution.

As seen from the above results, the ZnO/Au film with the ZnO:Au ratio equal to 1:2 manifests enough absorption for efficient removal of  $\text{Fe}^{2+}$ . In other words, a high reduction of  $\text{Fe}^{2+}$  concentration at this ratio allows one to transfer  $\text{Fe}^{2+}$  from the solution to the film. To confirm this important aspect, we check further on the surface morphology of our films. Fig. 10 illustrates the morphology of the films with different ZnO:Au ratios after the system has been removing the metal during 90 min. The ZnO nanoparticles (with the diameters  $50 \pm 5$  nm) looks uniform on the glass substrate (see a red arrow in Fig. 10). The additional Au amount (with the diameters  $100 \pm 10$  nm) in the ZnO nanoparticles also reveals uniformity on the substrate (see a blue arrow). As compared with the ZnO nanoparticles, the Au clusters are remarkably observed. It is partly due to size-dependent effect on the film formation. When one passes gradually from the ZnO:Au ratio 1:0 to 1:2, the additional amount of Au seems to increase cluster aggregation from small- to large-sized (see Fig. 10a, b, c and d). Furthermore, it would be natural to suggest that a clay-like colour scattering in these films originates from gradual formation of  $\text{Fe}^{2+}$ . In summary, the larger Au amount we add into the film, the more expressive process of  $\text{Fe}^{2+}$  formation on the film we obtain.

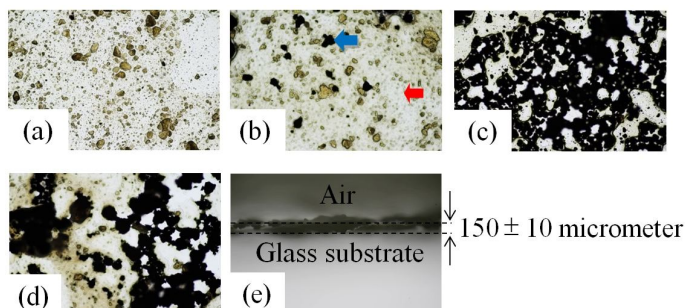


**Fig. 10.** Illustrations of surface morphology of our ZnO/Au films at different ZnO:Au ratios: (a) 1:0, (b) 1:0.5, (c) 1:1, and (d) 1:2, as observed after the system removes some metal. The thickness of all the films is  $150 \pm 10$   $\mu\text{m}$  (see panel e).

The photocatalytic efficiency of the ZnO/Au film can be improved using the two principal mechanisms, the surface plasmon resonance and the Schottky-barrier effect (see Fig. 11). Notice that here ZnO represents a semiconductor photocatalyst, while Au itself is a plasmonic crystal.

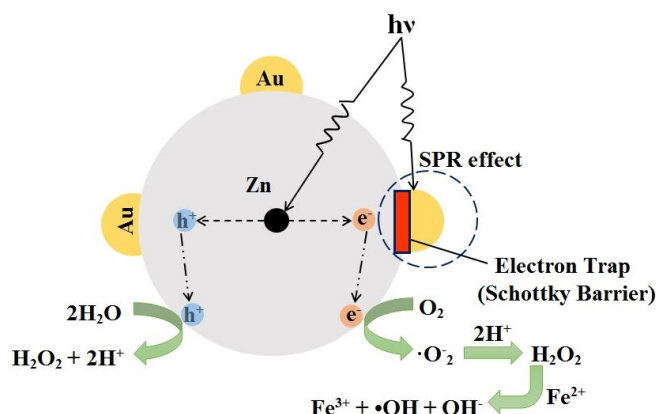
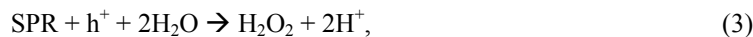


Fig. 11. Mechanism of photocatalytic efficiency of our ZnO/Au films.

It is well-known that coupling of the electric field and the free electrons from Au causes the surface plasmon resonance (SPR) [12]. On the other hand, the electrons from ZnO are excited from the valence band to the conduction one, thus generating electron–hole pairs according to the following scheme:



In cooperation with ZnO, Au strongly induces separation of the electron–hole pairs linked with ZnO:



Note that  $\cdot\text{O}_2^-$  represents a superoxide radical. Since the Fermi level of ZnO is higher than that of Au, the electrons in the conduction band of ZnO can possibly be transferred to the hot electrons from Au, which are in a close contact (see Fig. 12).

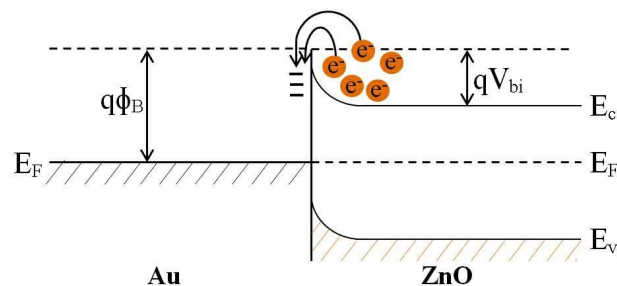
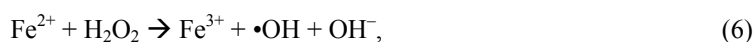


Fig. 12. Energy diagram of Au–ZnO interface:  $\Phi_B$  – Schottky-barrier height,  $V_{bi}$  – built-in potential,  $E_c$  – conduction-band energy,  $E_F$  – Fermi energy,  $E_v$  – valence-band energy, and  $q$  – electric charge.

Meanwhile, the localized electrons from Au cannot cross over the Schottky-barrier height of ZnO [11]. The confined electrons from Au are therefore trapped at the interface between ZnO and Au, resulting in a rapidly increasing separation rate for the electron–hole pairs. This induces broadening of the spectra from the ultraviolet towards the visible range, which occurs with

increasing Au amount in the ZnO matrix. The absorption-peak intensity of ZnO/Au film is then steadily improved.

Finally, high amounts of the electrons available at the interface between ZnO and Au react continuously with the ferrous ion:



where  $\cdot\text{OH}$  denotes a hydroxyl radical. Therefore, the photocatalytic performance of the ZnO/Au film is improved due to reduced amount of the ferrous form.

#### 4. Conclusion

The gold nanoparticles embedded into the zinc-oxide films have been fabricated using the spin-coating approach. Then the films have been dipped into the  $\text{Fe}^{2+}$  solution that serves as a model representative of metals in the wastewater, in order to detect their photocatalytic activity. It has been found that, due to the surface plasmon resonance and the Schottky-junction effect, the increased amount of gold nanoparticles in the ZnO matrix leads to broadening of the absorption spectrum. Moreover, this enhances the absorption-peak intensity in the visible-wavelength range. The ZnO:Au ratio 1:2 manifests a sufficient photocatalytic performance for removing  $\text{Fe}^{2+}$  at its initial concentration 0.2 mM. The higher the concentration of gold, the better the photocatalytic performance becomes. Of course, a material component of the cost of wastewater treatment has also to be taken into account. In particular, this is true when the excessive Au amounts must be applied to reduce the  $\text{Fe}^{2+}$  concentrations lower than the standard value of 0.2 mM.

#### Acknowledgement

This work was supported by the King Mongkut's Institute of Technology Ladkrabang, Bangkok 10520, Thailand.

#### References

1. Baruah S, Pal S K and Dutta J, 2012. Nanostructured zinc oxide for water treatment. *NanoSci. Nanotechnol. Asia*. **2**: 90–102.
2. Lu Y, Hao L, Hirakawa Y and Sato H, 2012. Antibacterial activity of  $\text{TiO}_2/\text{Ti}$  composite photocatalyst films treated by ultrasonic cleaning. *Adv. Mater. Phys. Chem.* **2**: 9–12.
3. Gupta K, Singh R P and Pandey A, 2013. Photocatalytic antibacterial performance of  $\text{TiO}_2$  and Ag-doped  $\text{TiO}_2$  against *S. aureus*, *P. aeruginosa* and *E. coli*. *Beilstein J. Nanotechnol.* **4**: 345–351.
4. Verdier T, Coutand M, Berton A and Roques C, 2014. Antibacterial activity of  $\text{TiO}_2$  photocatalyst alone or in coatings on *E. coli*: The influence of methodological aspects. *Coatings*. **4**: 670–686.
5. Lee W S, Park Y S and Cho Y K, 2015. Significantly enhanced antibacterial activity of  $\text{TiO}_2$  nanofibers with hierarchical nanostructures and controlled crystallinity. *Analyst*. **140**: 616–622.
6. Jeon S and Yong K, 2010. Morphology-controlled synthesis of highly adsorptive tungsten oxide nanostructures and their application to water treatment. *J. Mater. Chem.* **20**: 10146–10151.
7. Fraga L E and Zannoni M V B, 2011. Nanoporous of  $\text{W}/\text{WO}_3$  thin film electrode grown by electrochemical anodization applied in the photoelectrocatalytic oxidation of the basic red 51

- used in hair dye. J. Brazilian Chem. Soc. **22**: 718–725.
8. Joshi U A, Darwent J R, Yiu H H P and Rosseinsky M J, 2011. The effect of platinum on the performance of  $\text{WO}_3$  nanocrystal photocatalysts for the oxidation of methyl orange and isopropanol. J. Chem. Technol. Biotechnol. **86**: 1018–1023.
  9. Singh S, Srivastava V C and Lo S L, 2016. Surface modification or doping of  $\text{WO}_3$  for enhancing the photocatalytic degradation of organic pollutant containing wastewaters: A review. Mat. Sci. Forum. **855**: 105–126.
  10. Zhang X, Liu Y, Lee S-T, Yang S and Kang Z, 2014. Coupling surface plasmon resonance of gold nanoparticles with low photon effect of  $\text{TiO}_2$  photonic crystals for synergistically enhanced photoelectrochemical water splitting. Energy Environ. Sci. **7**: 1409–1419.
  11. Xianming H, 2014. Nonaqueous fabrication of ZnO/Au nanohybrids with enhanced photocatalytic activity. Mater. Lett. **137**: 319–322.
  12. Nayane U, Myeongsoon L, Junhyung K and Dongil L, 2011. Well-defined Au/ZnO nanoparticle composites exhibiting enhanced photocatalytic activities. ACS Appl. Mater. Interf. **3**: 4531–4538.
  13. Yiqiang S, 2016. Complete Au@ZnO core-shell nanoparticles with enhanced plasmonic absorption enabling significantly improved photocatalysis. Nanoscale **8**: 10774–10782.
  14. Ramanathan S. Thin film metal-oxides, 1st Ed. (New York: Springer, 2010).
  15. Locharoenrat K and Damrongsak P, 2015. Plasmonic properties of gold-palladium core-shell nanorods. Ukr. J. Phys. Opt. **16**: 120–126.

---

Thonglim P., Sirivichai M., Thanjai O. and Locharoenrat K. 2018. Removal of metals using a ZnO/Au composite under visible-light illumination. Ukr.J.Phys.Opt. **19**: 60 – 68.

**Анотація.** Наночастинки золота, вбудовані в плівку ZnO, виготовлено за допомогою простої технології покриття за методом центрифугування. Фотокаталітичні характеристики плівки вивчено за умови опромінення видимим світлом. Запропоновано збільшувати кількість наночастинок Au у матриці ZnO (у нашому конкретному випадку – від 0 до 400 мг) для поліпшення фотокаталітичної ефективності плівки, що досягають завдяки сукупній дії ефектів плазмонного резонансу та бар'єра Шотткі. У якості типового представника металів, наявних у стічних водах, обрано  $\text{Fe}^{2+}$ . Показано, що плівки ZnO/Au із підвищеним вмістом Au ефективно зменшують кількість іонів заліза у водному розчині. Зокрема, плівка зі співвідношенням вмісту ZnO: Au = 1:2 слугує хорошим поглиначем для видалення іонів  $\text{Fe}^{2+}$  у разі, якщо їхня початкова концентрація дорівнює 0,2 мМоль.